Enhancement of field–analyte interaction at metallic nanogap arrays for sensitive localized surface plasmon resonance detection

Rabiatul Adawiah Awang, Sherif Hamdy El-Gohary, Nak-Hyeon Kim, and Kyung Min Byun*

Department of Biomedical Engineering, Kyung Hee University, Yongin 446-701, South Korea

*Corresponding author: kmbyun@khu.ac.kr

Received 6 August 2012; revised 25 September 2012; accepted 26 September 2012; posted 28 September 2012 (Doc. ID 173911); published 22 October 2012

We investigated the near-field enhancement of a localized surface plasmon resonance (LSPR) structure based on gold nanograting pairs with a nanosized gap. The results calculated by finite-difference time-domain and rigorous coupled-wave analysis methods presented that the nanogap enclosed by two neighboring nanogratings produced significant confinement and enhancement of electromagnetic fields and allowed a sensitive detection in sensing of surface binding events. Gold gratings with a narrow gap distance less than 10 nm showed enhanced refractive index sensitivity due to the intensified optical field at the nanogap, outperforming the LSPR structure with noninteracting nanogratings. Also, we analyzed the effectiveness of using an overlap integral (OI) between analyte and local plasmon field to estimate the detection sensitivity. We found a strong correlation of field–analyte OI with far-field sensor sensitivity.

OCIS codes: 050.6624, 240.6680, 280.4788.

1. Introduction

Interest in biosensing devices has grown enormously over the past decade, with applications being found in such disparate areas as point-of-care clinical diagnosis, environmental protection, and food safety [1]. Progress in this field has been made with an aim of realizing high sensitivity, miniaturization, and multichannel and real-time detection. Among a wide variety of sensing approaches, optical biosensor has secured a very important place due to its rapid, noninvasive, and real-time monitoring capability [2]. More recently, label-free optical detection methods of perceiving biomolecular binding events without the need of external labels are gaining much attention as an alternative to fluorescence dyes that may suffer from toxicity and photobleaching [3].

The surface plasmon resonance (SPR) phenomenon has been heavily utilized as an efficient label-free optical sensing technique since its first introduction by Liedberg *et al.* in 1983 [4]. Owing to its ability of monitoring small changes at the metal–dielectric interface, SPR has worked as a sensitive reporter for biochemical reactions that influence the refractive index of the local environment of a probe. In general, a conventional SPR biosensor is based on Kretschmann's attenuated total reflection configuration [5]. Charge density oscillations known as surface plasmons (SPs) are highly excited at the surface of a metal film, when the SPs are resonantly coupled with incident photons. These plasmons propagate tens to hundreds of micrometers along the metal surface and also decay exponentially from the surface (perpendicular to the metal–dielectric interface) [6].

Contrary to propagating SP waves, nonpropagating localized SPR (LSPR) can be supported by

1559-128X/12/317437-06$15.00/0

metallic nanostructures. Since the spectral position of LSPR is tuned by adjusting the size and shape of the nanostructures, recent advance of fabrication techniques allows the LSPR properties to be manipulated effectively in the nanoscale domain [7]. In particular, near-field interaction between two or more nanostructures separated by a very small gap, typically within the decay length of ~10 nm, has been studied intensively because the coupling between individual LSPR modes may lead to a new hybridized plasmon mode, leading to strong electromagnetic field confinement and enhancement within the gap [8]. Hence, there has been a growing interest in LSPR sensing of biomolecules using a nanostructured substrate, such as nanoparticle or nanogap arrays, in the pursuit of single-molecule detection [9]. However, while investigations on the near-field characteristics, for example, hot-spot generation [10] and distance dependence of plasmon coupling [11], have been well established, a detailed description on the effect of near-field interaction with analytes on the LSPR sensor sensitivity still remains unclear, especially at the nanogap array structure.

In this study, we intend to demonstrate how the near-field coupling in the nanosized gap can affect the LSPR biosensing performance in the far field. The results will elucidate the correlation between the gap distance and the sensitivity of LSPR biosensor in a quantitative way. This study suggests that metallic nanogap arrays can be promising for sensitive LSPR detection of biointeractions.

2. Numerical Model

LSPR configuration with interacting nanograting pairs is shown in Fig. 1. We assume one-dimensional gold nanogratings built on a high-index SF10 glass substrate in an ambience of phosphate buffered saline (PBS) solution. Individual rectangular nanograting has a width of $w = 20$ nm and a height of $h = 20$ nm, and the two interacting elements are separated by a distance g. For individual internanograting separation of $g = 30$, 20, 10, 7, and 5 nm, we observe the near- and far-field characteristics when the period Λ, defined as a distance between the nanograting pairs, is fixed at $\Lambda = 100$ nm. The above geometric parameters were chosen based on the previous numerical and experimental studies on sensitive LSPR detection [12,13] and the feasibility in actual implementation [14]. It should be noted that maximum gap distance is 30 nm and nearly touching nanogratings of $g < 5$ nm are not considered because multiple side lobes appear in an extinction spectrum as a result of higher-order near-field interactions. Moreover, since those extremely narrow gaps show an unexpected plasmonic behavior of anomalous dispersion [15], which can give rise to a reversal of spectral shift in the resonance wavelength, this blueshift effect will be covered in our subsequent study.

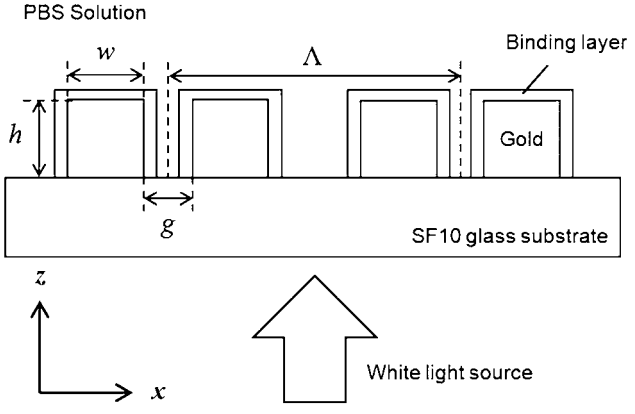

Fig. 1. Schematic diagram of the proposed LSPR configuration. One-dimensional gold nanograting pairs with a nanogap g and a period Λ are regularly patterned on a SF10 glass substrate. The white light source of TM polarization is normally incident to the glass substrate. An individual gold grating is presumed to have a height of $h = 20$ nm and a width of $w = 20$ nm. Binding analytes are modeled as a 1 nm thick dielectric monolayer that uniformly covers the gold nanogratings in PBS solution.

For the proposed LSPR structure, potential use of interest is to sense the change in the concentration of biomolecules adsorbed onto the metallic nanogratings. In order to determine the sensor sensitivity, biointeractions are presumed to take place within a 1 nm thick homogeneous layer, and the LSPR spectrum is calculated as its refractive index changes gradually from 1.33 (index of PBS solution) to 1.60 due to the molecular adsorption on the sensor surface. Also, we assume that a white light source with a transverse-magnetic (TM) polarization, the electric field of which oscillates in parallel to the grating vector, is normally incident to the substrate. The frequency-dependent permittivities of SF10 and gold are taken from [16].

In the case of a metallic nanostructure-based LSPR system, it is difficult to compare the near-field distribution and the sensor sensitivity directly using analytical approaches. We have thus employed finite-difference time-domain (FDTD) and rigorous coupled-wave analysis (RCWA) methods for numerical computation of near-field and far-field characteristics. FDTD calculation shows two-dimensional electromagnetic field components of E_X, H_Y, and E_Z near the substrate when a TM-polarized light is incident. Much theoretical and experimental literature has demonstrated that interacting or noninteracting nanostructures associated with localized plasmons confined within a nanoscale boundary can be numerically calculated by using the FDTD method [13,17,18]. On the other hand, RCWA has been successfully applied to predict far-field optical characteristics produced by periodic nanopatterns [19,20]. This method is based on a complete solution of Maxwell's equations in a film structure composed of periodic layers [21,22]. An appropriate number of space harmonic orders is determined to be 30, which is sufficient to support the accuracy and convergence of our RCWA calculations.

3. Results and Discussion

As a quantitative measure of the LSPR response, optical extinction is defined as $-\log(T)$, where T denotes the zeroth-order transmittance as a function of wavelength when assuming that the light source is a unit-amplitude plane wave. Figure 2 shows extinction spectra for various gap distances. It is important to note that the plasmon resonance strongly redshifts as the gap is reduced. Such spectral behavior is well consistent with the previous observation by other groups. Based on the dipole–dipole coupling model [23], Jain *et al.* demonstrated that a dipole–dipole interaction of Au nanodisc pairs is attractive for TM polarization, which leads to the reduction of the plasmon frequency (i.e., redshift of the LSPR wavelength) [11]. In Fig. 2, the interactions between neighboring nanogratings are clearly stronger with a decreased gap distance as seen from larger wavelength shifts.

Using the results of Fig. 2, we compute the shift in extinction maximum wavelength, i.e., $\Delta\lambda_{\mathrm{LSPR}} = \lambda_{\mathrm{LSPR}} - \lambda_0$, as a function of gap size. In Fig. 3, the LSPR wavelength for $g = 30$ nm has been used as a reference λ_0 for calculation of $\Delta\lambda_{\mathrm{LSPR}}$ owing to its minimum coupling effect. Obviously, the plasmon shift tends to follow an exponential decay. The red curve implies a least-square fit to the first-order exponential function $y = y_0 + A\exp(-x/l)$, yielding $y_0 = 0$, $A = 21.58 \pm 6.72$ nm, a decay length $l = 4.32 \pm 0.96$ nm, and $R^2 = 0.969$. Although the plot does not include the data points at which the nanogratings are nearly touching, because of the presence of higher-order resonances and anomalous dispersion, the LSPR shift increases exponentially with a decreasing gap.

In order to visualize an effect of near-field interaction, we have characterized the field distributions using FDTD methods. The plots in Fig. 4 show the electric field profiles across the surface of the LSPR

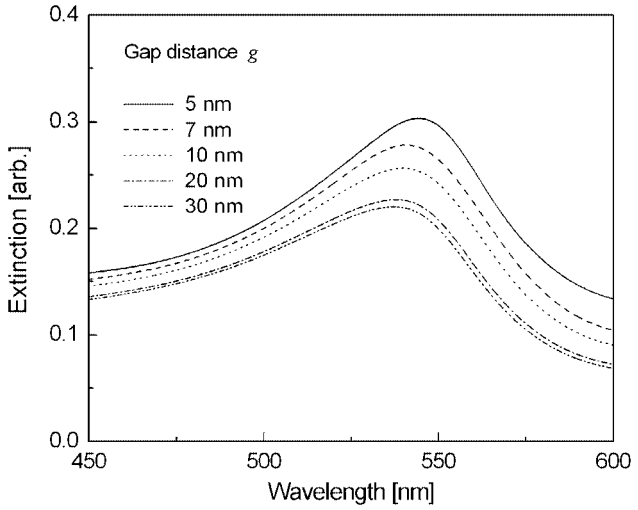

Fig. 2. RCWA results of extinction spectra when a gap distance varies from 5 to 30 nm. The refractive index of a binding layer is 1.33.

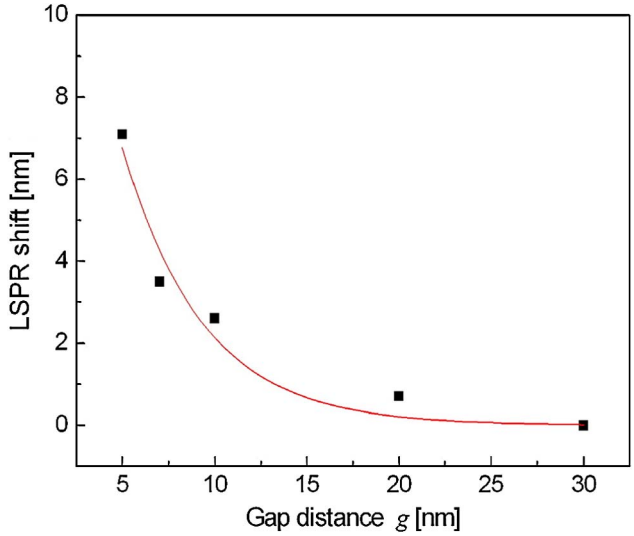

Fig. 3. (Color online) Shift in the plasmon wavelength of gold nanograting pair as a function of the gap distance. The red curve is the least-squares fit to the first-order exponential function.

structure at a gap of $g = 30$ nm. The metallic nanogratings redistribute the plasmon waves such that the field is perfectly symmetric and higher field amplitude is found at the grating corners. Primary peaks with the strongest amplitudes are located on the two lower edges of the nanograting and the secondary peaks on the upper sides. On the assumption of an incident light of unit amplitude, the maximum field amplitude obtained is $E_X = 11.2$. Since the amplitude of locally enhanced plasmon decays abruptly away from the grating surface, individual plasmon peaks associated with the four grating corners can be regarded as resonant LSPR modes. However, relatively large gap size, compared with the decay length of the LSPR mode, makes the field enhancement at the nanogap region less significant.

On the other hand, for a smaller gap of $g = 5$ nm, a fairly enhanced field is found in the nanogap region enclosed by the two separate nanogratings as shown in Fig. 5. While the maximum enhancement of 13.8 times the incident light amplitude obtained at the lower edges is not much greater than the case of $g = 30$ nm, a note worth a look is that large field amplification over 4 times can be achieved within the nanogap region. This is particularly advantageous in designing a high-sensitivity LSPR biosensor with large and effective binding sites because it cannot be easily confirmed if the sharp edges really exist in the fabricated nanostructures [8]. Even if implementation of LSPR substrates with sharp tips is technically possible, target localization into such narrow regions with a highly enhanced field are essential for preventing the biomolecules from being wasted in the weak field [24]. As a result, LSPR structure with a large volume of relatively high field intensity can be a promising candidate to solve the limitations of a traditional LSPR system.

Although the results are not shown here, FDTD computations for the gap distance less than 5 nm

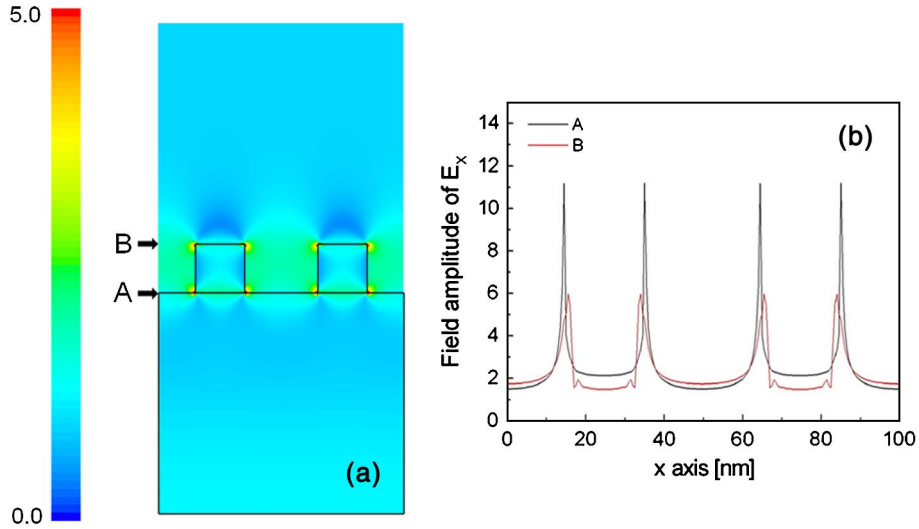

Fig. 4. (Color online) FDTD results of the LSPR structure with a gap of $g = 30$ nm. (a) The near-field distribution image is normalized by the field amplitude of 5. (b) Horizontal field distributions of E_X show individual LSPR modes and the field profiles at the nanogap region.

presented a more enhanced field at the nanogap, and such enhancement is comparable to the LSPR modes at the grating corners. Therefore, we believe that there is more room for additional optimization of geometric parameters of gold nanogratings for obtaining stronger field enhancement. However, fabricating the optimized LSPR structures in a reproducible manner and guiding biointeractions into the extremely narrow gap still remains a challenge.

As an example of actual application of the proposed LSPR configuration, rectangular gold nanograting pairs are applied as an LSPR biosensor to detect biomolecular interactions occurring at the grating surface. As mentioned in Section 2, target binding is modeled as a 1 nm thick dielectric monolayer whose refractive index changes from 1.33, i.e., no target analytes in water solutions, to 1.60 in accordance with the concentration of adsorbed analytes. In Fig. 6, when $g = 10$ nm, the plasmon wavelength tends to redshift progressively because the resonance wavelength is sensitive to the local change in the environment surrounding the gold grating. The sensitivity, i.e., the slope of the resonance wavelength over the refractive index range, is found to be 14.1 nm/RIU, where RIU stands for refractive index unit. Interestingly, it is noteworthy that this far-field characteristic of sensor sensitivity can be adjusted by controlling the gap distance. Since a higher field enhancement in the nanogap can be accomplished by a smaller gap size, target analytes adsorbed at the nanogap region tend to participate more vigorously on average than those on the other grating regions, finally leading to a better sensitivity for narrower gap distance.

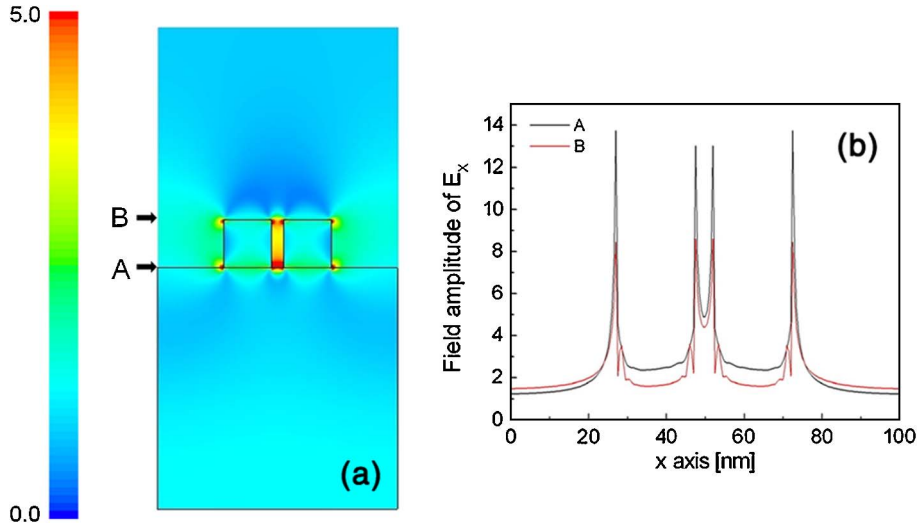

Fig. 5. (Color online) FDTD results of the LSPR structure with a gap of $g = 5$ nm. (a) The near-field distribution image is normalized by the field amplitude of 5. (b) Horizontal field distributions of E_X show enhanced field amplitudes at the nanogap, compared with the results in Fig. 4.

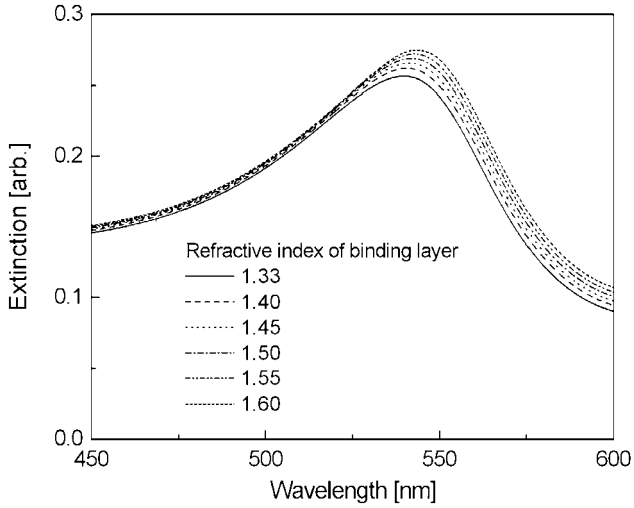

Fig. 6. Extinction spectra of the gold nanograting pairs with $g = 10$ nm as the refractive index of a binding layer increases from 1.33 to 1.60.

Figure 7 presents the sensitivity characteristic of the LSPR structure when a nanogap is varied from 5 to 30 nm. The refractive index change occurring at $g = 5$ nm produces the highest refractive index sensitivity of 20.7 nm/RIU, showing 65% improvement in sensitivity compared with the case of $g = 30$ nm. It is thus obvious that the local field enhancement at the smaller gap makes more significant contribution to achieving a higher sensitivity. On the other hand, the gold nanograting pairs with a relatively large separation over 20 nm cannot generate an additional improvement in sensitivity due to the minimum coupling effect between LSPR modes. Subsequently, in order to verify the correlation between the refractive index sensitivity and the local plasmon field, an overlap integral (OI) has been introduced [25]. We define an OI of field intensity as given by

$$\mathrm{OI} = \frac{1}{\Lambda}\int_{x=0}^{x=\Lambda}\int_{z=0}^{z=\infty} \Delta n(x,z)\cdot|\mathrm{E_X}(x,z)|^2 \mathrm{d}z\mathrm{d}x, \qquad (1)$$

where x and z represent the horizontal and vertical axes in Fig. 1. Among three nonzero field components of E_X, H_Y, and E_Z for TM polarization, the highest correlation between the field–matter overlap and the sensor sensitivity was obtained with the intensity of E_X [26]. $\Delta n(x,z)$ is a refractive index change caused by the binding event of target molecules, and thus, $\Delta n(x,z) = 0.27$ within the 1 nm thick binding layer, and otherwise $\Delta n(x,z) = 0$.

As the OI is highly associated with the field enhancement at the analyte region, calculation results in Fig. 7 clearly show a rapid increment with a decreasing gap distance. When the two parameters are respectively normalized by the maximum values of 20.7 nm/RIU and OI = 2071 at $g = 5$ nm and compared directly, it is found that the sensitivity is greatly in accord with the OI. The quantification of near-field enhancement behavior allows us to derive an OI that gives an estimate of the far-field sensitivity. In other words, this proof-of-concept study shows an interesting possibility that an evaluation of near-field quantity can be used to estimate the far-field performance. Summarizing the results, we suggest that one can significantly improve the sensitivity of LSPR biosensor by introducing the immobilization of specific probes such as DNA, antibodies, or oligonucleotides onto the specific gap area between the nanogratings, which has been recognized as to have the most sensitivity properties.

In the final part of discussion, we present a brief investigation in terms of the linearity, which is another important sensing performance. For the proposed LSPR structure of $g = 5$ nm, Fig. 8 shows that the resonance wavelength shifts linearly for a wide refractive index change of the binding sites. Since a linear relationship is evident with a correlation coefficient $R = 0.9999$, the nanogap-based LSPR

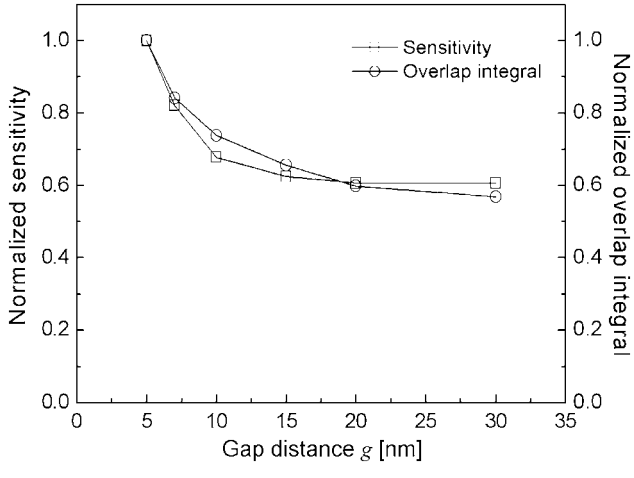

Fig. 7. Correlation analysis between the sensor sensitivity and the OI as a function of gap distance. The sensitivity and OI are normalized by the maximum values of 20.7 nm/RIU and 2071, respectively.

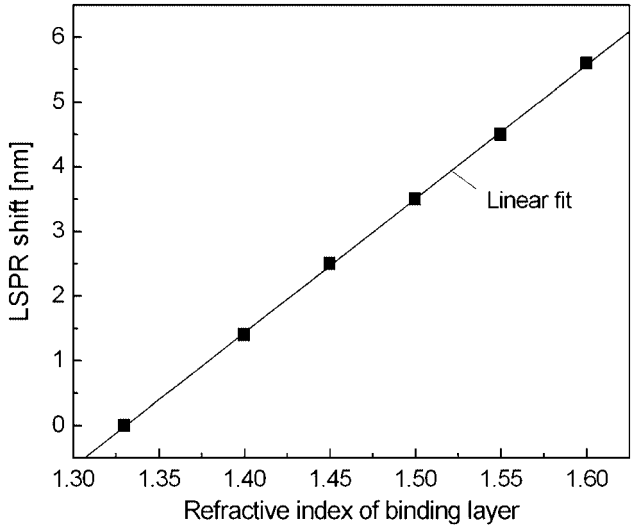

Fig. 8. Linear sensing performance of the proposed LSPR structure at a gap of $g = 5$ nm.

structure is potentially useful in realizing an effective LSPR detection with high sensitivity and a great linearity in a wide dynamic range.

4. Conclusion

In this study, nanogap array-based LSPR structure has been designed by introducing gold nanograting pairs with a nanosized gap. While near-field coupling between the two nanogratings may yield an exponential change of LSPR characteristic, the field enhancement at the nanogap contributed greatly to an improvement of sensor sensitivity, especially when a binding event occurs at the nanogap region. Moreover, when analyzing the sensor sensitivity quantitatively, there was a strong correlation between the sensitivity and the OI. This was found to be due to the generation of enhanced field intensity within the nanogap region. Since an extremely narrow gap tends to produce an enormous field enhancement associated with a new hybridized LSPR mode while it is not easy to guide biointeractions into such regions, an additional optimization of nanogap geometry is possible. Therefore, it is believed that the OI can be a useful tool to assess the performance of emerging LSPR sensors that address enhancement of detection sensitivity. Fabrication of devices following the proposed LSPR design is currently underway with a help of nanoimprint lithographic technique [27,28].

This research was supported by the Kyung Hee University research fund in 2011 (KHU-20110455).

References

1. V. Scognamiglio, G. Pezzotti, I. Pezzotti, J. Cano, K. Buonasera, D. Giannini, and M. T. Giardi, "Biosensors for effective environmental and agrifood protection and commercialization: from research to market," Microchim. Acta **170**, 215–225 (2010).
2. F. S. Ligler, "Perspective on optical biosensors and integrated sensor systems," Anal. Chem. **81**, 519–526 (2009).
3. X. Fan, I. M. White, S. I. Shopova, H. Zhu, J. D. Suter, and Y. Sun, "Sensitive optical biosensors for unlabeled targets: a review," Anal. Chim. Acta **620**, 8–26 (2008).
4. B. Liedberg, C. Nylander, and I. Lunstrom, "Surface plasmon resonance for gas detection and biosensing," Sens. Actuators **4**, 299–304 (1983).
5. J. Homola, "Present and future of surface plasmon resonance biosensors," Anal. Bioanal. Chem. **377**, 528–539 (2003).
6. A. W. Wark, H. J. Lee, and R. M. Corn, "Long-range surface plasmon resonance imaging for bioaffinity sensors," Anal. Chem. **77**, 3904–3907 (2005).
7. M. E. Stewart, C. R. Anderton, L. B. Thompson, J. Maria, S. K. Gray, J. A. Rogers, and R. G. Nuzzo, "Nanostructured plasmonic sensors," Chem. Rev. **108**, 494–521 (2008).
8. S. Wang, D. F. P. Pile, C. Sun, and X. Zhang, "Nanopin plasmonic resonator array and its optical properties," Nano Lett. **7**, 1076–1080 (2007).
9. J. N. Anker, W. P. Hall, O. Lyandres, N. C. Shah, J. Zhao, and R. P. van Duyne, "Biosensing with plasmonic nanosensors," Nat. Mater. **7**, 442–453 (2008).
10. T. Chung, S.-Y. Lee, E. Y. Song, H. Chun, and B. Lee, "Plasmonic nanostructures for nano-scale bio-sensing," Sensors **11**, 10907–10929 (2011).
11. P. K. Jain, W. Huang, and M. A. El-Sayed, "On the universal scaling behavior of the distance decay of plasmon coupling in metal nanoparticle pairs: a plasmon ruler equation," Nano Lett. **7**, 2080–2088 (2007).
12. K. Kim, D. J. Kim, S. Moon, D. Kim, and K. M. Byun, "Localized surface plasmon resonance detection of layered biointeractions on metallic subwavelength nanogratings," Nanotechnology **20**, 315501 (2009).
13. N.-H. Kim, W. K. Jung, and K. M. Byun, "Correlation analysis between plasmon field distribution and sensitivity enhancement in reflection- and transmission-type localized surface plasmon resonance biosensors," Appl. Opt. **50**, 4982–4988 (2011).
14. X. Liang, K. J. Morton, R. H. Austin, and S. Y. Chou, "Single sub-20 nm wide, centimeter-long nanofluidic channel fabricated by novel nanoimprint mold fabrication and direct imprinting," Nano Lett. **7**, 3774–3780 (2007).
15. Y. S. Jung, J. Wuenschell, H. K. Kim, P. Kaur, and D. H. Waldeck, "Blue-shift of surface plasmon resonance in a metal nanoslit array structure," Opt. Express **17**, 16081–16091 (2009).
16. E. D. Palik, *Handbook of Optical Constants of Solids* (Academic, 1985).
17. Y. Liu, R. Cheng, L. Liao, H. Zhou, J. Bai, G. Liu, L. Liu, Y. Huang, and X. Duan, "Plasmon resonance enhanced multicolour photodetection by graphene," Nat. Commun. **2**, 579 (2011).
18. Y. Chu, E. Schonbrun, T. Yang, and K. B. Crozier, "Experimental observation of narrow surface plasmon resonances in gold nanoparticle arrays," Appl. Phys. Lett. **93**, 181108 (2008).
19. Y. Kanamori, K. Hane, H. Sai, and H. Yugami, "100 nm period silicon antireflection structures fabricated using a porous alumina membrane mask," Appl. Phys. Lett. **78**, 142 (2001).
20. Q. Cao and P. Lalanne, "Negative role of surface plasmons in the transmission of metallic gratings with very narrow slits," Phys. Rev. Lett. **88**, 057403 (2002).
21. M. G. Moharam and T. K. Gaylord, "Rigorous coupled-wave analysis of metallic surface-relief gratings," J. Opt. Soc. Am. A **3**, 1780–1787 (1986).
22. L. Li and C. W. Haggans, "Convergence of the coupled-wave method for metallic lamellar diffraction gratings," J. Opt. Soc. Am. A **10**, 1184–1189 (1993).
23. W. Rechberger, A. Hohenau, A. Leitner, J. R. Krenn, B. Lamprecht, and F. R. Aussenegg, "Optical properties of two interaction gold nanoparticles," Opt. Commun. **220**, 137–141 (2003).
24. K. M. Byun, S. M. Jang, S. J. Kim, and D. Kim, "Effect of target localization on the sensitivity of a localized surface plasmon resonance biosensor based on subwavelength nanostructures," J. Opt. Soc. Am. A **26**, 1027–1034 (2009).
25. A. Shalabney and I. Abdulhalim, "Electromagnetic fields distribution in multilayer thin film structures and the origin of sensitivity enhancement in surface plasmon resonance sensors," Sens. Actuators A **159**, 24–32 (2010).
26. W. Lee and D. Kim, "Field–matter integral overlap to estimate the sensitivity of surface plasmon resonance biosensors," J. Opt. Soc. Am. A **29**, 1367–1376 (2012).
27. A. Boltasseva, "Plasmonic components fabrication via nanoimprint," J. Opt. A **11**, 114001 (2009).
28. S.-W. Lee, K.-S. Lee, J. Ahn, J.-J. Lee, M.-G. Kim, and Y.-B. Shin, "Highly sensitive biosensing using arrays of plasmonic Au nanodisks realized by nanoimprint lithography," ACS Nano **5**, 897–904 (2011).